Shilin LIU[1,2], Jinyu WEN[1], Shaorong WANG[1]

Huazhong University of Science and Technology (1), West Anhui University (2)

Novel configuration and control of DFIG-based FESS associated to a wind turbine connected to power grid

Abstract. *The power output of wind turbine (WT) is unpredicted and irregular, large scale wind power integrated to power grid influences the power system stability heavily. The multi-functional flexible power conditioner (FPC) is a flywheel energy storage system (FESS) based on doubly-fed induction generator (DFIG), which can perform functions including energy storage, active and reactive power generation. To enhance the power output characteristics of WT, a novel configuration of FPC associated to WT (WT-FPC) is proposed. According to the configuration and control targets of WT-FPC, the control strategies are studied. The active power of the associated system is regulated based on a fuzzy logic inference system, and machine terminal voltage was controlled by regulating the reactive power of FPC. The model of WT-FPC is established and the time-domain simulations are performed using MATLAB/Simulink. The simulation results show the feasibility and effectiveness of the proposed WT-FPC and its control strategies, and the operation characteristics of the WT connected to the grid are enhanced evidently.*

Streszczenie. *Moc wyjściowa turbiny wiatrowej jest nieregularna i trudna do przewidzenia. W celu poprawy charakterystyki mocy turbiny wiatrowej zaproponowano nowy układ FPC (flexible power conditioner). Do sterowania mocą czynną użyto regulatora z logiką rozmytą a napięcie wyjściowe było sterowane przez kontrolę mocy biernej. (**Nowy system sterowania generatorem DFIG w turbinie wiatrowej dołączonej do sieci mocy**)*

Keywords: wind turbine, flexible power conditioner (FPC), fuzzy logic inference system, machine terminal voltage control
Słowa kluczowe: turbina wiatrowa , układ FPC – flexible power conditioner

1 Introduction

In the recent years, there have been an extensive growth and quick development in the exploitation of wind energy. As we know, the power output of wind turbine is always fluctuating with time and lack of controllability due to the inherent random characteristics of wind speed. With the number and capacity of wind turbines connected to the power grid increasing, the fluctuating power has adverse impacts on the stability and power quality of the connected power systems. For the energy storage systems (ESSs) can regulate the active and reactive power simultaneously and respectively, they are usually associated with the WTs, balancing the active and reactive power between generation and consumption [1]. Then the ESSs can be concerned with the main voltage and frequency control, and the WTs with ESSs can contribute to the ancillary services.

The ESSs include lead-acid battery, super-capacitor, superconducting magnetic energy storage (SMES), flywheel energy storage system (FESS), and so on. Nowadays, FESS has become the most popular energy storage system because of advances in power electronics, materials and magnetic bearings [2]. The advantages of FESS against other ESSs are no hazardous chemicals, long life, low maintenance costs, and insensitivity to environmental conditions [2-5]. FESS is capable of power cycles from seconds to a few minutes, and has been applied with some amount of success, typically, in wind power generation, automotive, and aerospace applications [6-10]. In addition, literature [11] shows that FESS is the most economical energy storage system if the maximum power cycle is 10 min.

Generally, the FESSs include high-speed and low-speed types. High-speed FESS running in a vacuum have a superior energy density but low power rating which is limited by cost and the difficulty of cooling [12]. Low-speed FESS, rated at hundreds of megawatts, has been used in high-energy physics facilities, and they can operate in air [13,14]. Cost is a concern for the power electronic converter used to interface the flywheel-coupled machine to the grid. To save on the converter cost, a doubly-fed induction machine (DFIG) is possible to be adopted [15]. The stator windings of the machine are directly connected to the grid, while the rotor windings are fed from the converter which only handles the rotor power, and the four-quadrant converter also recovers power between the machine and power grid [16]. Theoretically, a speed range of ±30% around the synchronous speed allows 71% of the maximum kinetic energy stored in the flywheel to be used for dynamic control, while the rotor converter is only rated at 23% of the total peak power including the stator and rotor power [13]. This configuration was previously exploited in industry for standby supplies [7], and literature [15] reports a study on the control of a 20-MW 200-MJ system to smooth the pulsating demand of a synchrotron.

For variable-speed power generation can enable operation of the turbine at its maximum power coefficient over a wide range of wind speeds, it's popular in current wind farms. One of the problems associated with variable-speed wind systems today is the presence of the gearbox coupling the wind turbine to the generator. This mechanical element suffers from considerable faults and increases maintenance expenses [17], so the direct-driven permanent magnet synchronous generator (PMSG) without gearbox is more and more attractive.

In this paper, the DFIG-based FESS, here called the flexible power conditioner (FPC), is used for smoothing the power output of wind turbine based on PMSG. Considering the cost of converters, a novel configuration of FPC associated to wind turbine (WT-FPC) is proposed. According to the configuration and the control targets of it, the control strategies are studied. The active power of the associated system is regulated based on a fuzzy logic inference system, and the machine terminal voltage is controlled by regulating the reactive power of FPC.

2 Modeling of the studied system

2.1 System configuration

Fig. 1 shows the configuration of the studied system which is consisted of a WT, a FPC, an AC bus, a transmission line, a local load, and an infinite power grid. The wind turbine is connected to the AC bus through a pair of full-power back-to-back converters. The FPC consists of a DFIG coupled with a large-inertia flywheel. The stator windings of FPC are connected to the AC bus directly, and the rotor side converter is connected to the DC-link of the WT's converters. The local load is connected to the AC bus, and the AC bus is integrated to the infinite bus through a transformer and a transmission line.

The main functions of FPC are reducing the fluctuation of power output and maintaining the stability of the terminal voltage, so the functions of the converters in the system defined as follow. (1) The wind turbine side converter (WSC) is controlled to obtain the optimal operation of the

turbine at its maximum power coefficient by maximum power point tracking (MPPT) control strategy, obtaining the largest energy capture from the wind. (2) The grid side converter (GSC) is controlled to maintain the stability of DC-link voltage by unity power factor control strategy. (3) The rotor side converter (RSC) provides the AC excitation to DFIG, controlling the active and reactive power of FPC. In this paper, the impact of switches and the detailed model of converters are not considered.

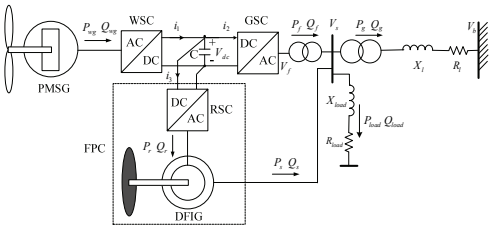

Fig.1. Configuration and power relation of WT-FPC

2.2 Modeling of wind turbine with PMSG

Simulation of the realistic response of the wind turbine with PMSG requires the modeling of the main electrical and mechanical components. The components considered include turbine, drive train and generator. The components are well established in the literature [17] and [18], however, for the sake of completeness of the paper, they are introduced in brief later.

The equations of the generator are projected on a reference coordinate system *dq* rotating synchronously with the magnet flux. The dynamic model of the surface-mounted PMSG in the magnet flux reference system is

$$\begin{cases} L_w \dfrac{di_d}{dt} = -u_d + L_w \omega i_q - R_{sw} i_d \\ L_w \dfrac{di_q}{dt} = -u_q - L_w \omega i_d + \omega \psi_w - R_{sw} i_q \end{cases} \tag{1}$$

where L_w and R_{Sw} are the generator inductance and resistance, respectively, ω is the generator electrical angular speed, and ψ_w is the magnet flux. This model adopts the generator convention, meaning that current is positive when flowing out of the generator. The electromagnetic torque is given by

$$T_{ew} = \frac{3}{2} p_w i_q \psi_w \tag{2}$$

where p_w is the pole-pair number. The dynamic of the drive train system can be expressed by the following equation,

$$T_{ew} - T_{mw} = \frac{J_w}{p_w} \dot{\omega} + M_w \omega \tag{3}$$

where J_w is the rotating inertia of the equivalent lumped masses, M_w is the friction damping coefficient, T_{mw} is the mechanical torque, which is determined by the captured wind power. T_{mw} is given by [18]

$$T_{mw} = \frac{0.5 \rho S V_w^3 C_p(\lambda_i, \beta)}{\omega_t} \tag{4}$$

where ρ is the air density, S is the blade impact area, V_w is the wind velocity, ω_t is the turbine speed, and C_p is the power coefficient of turbine, which can be expressed by

$$C_p(\lambda_i, \beta) = c_1 \left(\frac{c_2}{\lambda_i} - c_3 \beta - c_4 \beta^{c_5} - c_6\right) e^{-\frac{c_7}{\lambda_i}} \tag{5}$$

in which

$$\lambda_i = \left(\frac{1}{\lambda + c_8 \beta} - \frac{c_9}{\beta^3 + 1}\right)^{-1} \tag{6}$$

$$\lambda = \frac{R \omega_t}{V_w} \tag{7}$$

where β is the blade pitch angle of wind turbine, R is the blade's radius, λ is the tip speed ratio of wind turbine, c_1~c_9 are the constant coefficients for C_p, and λ_i is the intermediate variables.

2.3 Modelling of FPC

For the flywheel is driven by DFIG, the modeling of FPC can refer to the modeling of wind power generator with DFIG, the main difference between the two models is the rotor dynamic equation, for FPC, the mechanical torque T_m=0, but for wind power generator, it determined by the wind energy captured by turbine. For the electromagnetic behaviours in the stator are much faster than those in the rotor and have little effect on the machine's transient stability, it is neglected here. Adopting the generator convention, the following set of dynamic equations results [19],

$$\begin{cases} u_{sd} = -R_s i_{sd} + \omega_1 \psi_{sq} \\ u_{sq} = -R_s i_{sq} - \omega_1 \psi_{sd} \\ u_{rd} = R_r i_{rd} + \dfrac{\partial \psi_{rd}}{\partial t} - s \omega_1 \psi_{rq} \\ u_{rq} = R_r i_{rq} + \dfrac{\partial \psi_{rq}}{\partial t} + s \omega_1 \psi_{rd} \end{cases} \tag{8}$$

where R is the resistance, ψ is the flux linkage, ω_1 is the synchronous electrical angular speed, s is rotor slip. Subscripts s and r indicate stator and rotor quantities respectively.

The flux linkages in Eq. (8) can be calculated using the following set of equations,

$$\begin{cases} \psi_{sd} = L_s i_{sd} - L_m i_{rd} \\ \psi_{sq} = L_s i_{sq} - L_m i_{rq} \\ \psi_{rd} = L_r i_{rd} - L_m i_{sd} \\ \psi_{rq} = L_r i_{rq} - L_m i_{sq} \end{cases} \tag{9}$$

where L_m is the mutual inductance, L_s and L_r are the stator and rotor leakage inductances respectively. The dynamic of rotor can be expressed by the following equation,

$$-T_e = \frac{J_f}{p_f} \frac{d\omega_{rf}}{t} + \frac{M_f}{p_f} \omega_{r_f} \tag{10}$$

where ω_{rf} is the rotor electrical angular speed, p_f is the number of pole-pairs, M_f the friction damping coefficient. The electromagnetic torque T_e can be calculated by

$$T_e = p_f L_m (i_{sq} i_{rd} - i_{sd} i_{rq}) \tag{11}$$

The active and reactive power absorbed or released by FPC can be expressed by

$$\begin{cases} P_s = u_{sd} i_{sd} + u_{sq} i_{sq} \\ Q_s = u_{sq} i_{sd} - u_{sd} i_{sq} \end{cases} \tag{12}$$

$$\begin{cases} P_r = u_{rd} i_{rd} + u_{rq} i_{rq} \\ Q_r = u_{rq} i_{rd} - u_{rd} i_{rq} \end{cases} \tag{13}$$

2.4 Interfacing with power grid and local load

The voltage equation describing the interface with the external system can be expressed as

$$\dot{u}_s - \dot{u}_b = \left[\frac{P_g + jQ_g}{\dot{u}_s}\right]^* (R_l + jX_l) \tag{14}$$

where X_l and R_l are the tie-line reactance and resistance respectively, P_g and Q_g are the active and reactive power of WT-FPC delivered to power grid respectively, $\dot{u}_b$ and $\dot{u}_s$ are the voltage vectors of the external bus and the machine terminal bus respectively, and the external bus is defined as an infinite bus system. The voltage equation of local load is similar to Equ.14.

3 Control strategy for the converters

For the WSC is in charge of the optimal operation of WT and not the focus of this paper, it is not discussed in detail here. The controllers for RSC and GSC are described as follow.

3.1 Controller for RSC

The main task of RSC is controlling the active and reactive power absorbed or released by FPC. The control system is composed of three-level controllers: upper-level controller (UC), middle-level controller (MC), and bottom-level controller (BC). The UC calculates the active and reactive power exchanged between the FPC and the connected power gird according to the operation state of WT, and gives the power set points to the middle level controller. Using a suitable vector control strategy, the MC calculates the three-phase excitation voltage of variable frequency and amplitude for the DFIG, so as to decouple control of the active and reactive powers. The BC performs the PWM technology-based excitation control. The control block diagram of the RSC is shown in Fig.2. This paper mainly focuses on the external behavior of the FPC, and the controller for MC and BC is well done in other literatures, so only the detailed design of the UC is discussed here.

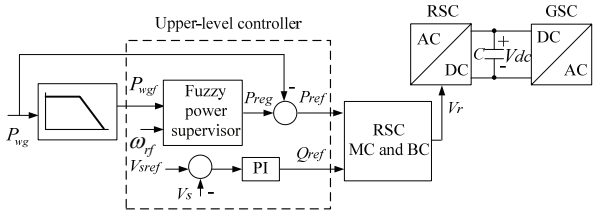

Fig.2. Control block diagram for the RSC

A. UC for the active power

If P_{reg} and P_{wg} represent the active powers expected from the coupling WT-FPC and generated by the WT, neglecting the power loss in converters, the reference value of the total active power P_{ref} (including stator and rotor sides) exchanged between the FPC and power grid can be expressed as

$$P_{ref} = P_{reg} - P_{wg} \tag{15}$$

From the Equ.15, we can get that P_{ref} should be identical with P_{wg} ideally, if P_{reg} is given already. But that means an infinite inertia of the flywheel in order to hamper the over-fulfillment of its speed limits. So a fuzzy logic power supervisor is applied to calculate the optimized value of P_{reg} [20]. The power supervisor adapts P_{reg} in function of ω_{rf} and P_{wgf}, which is the filtered value of P_{wg}. That is, the inputs of the fuzzy logic inference system are the filtered value of P_{wg} and the flywheel rotational speed ω_{rf}, and the output is the reference value P_{reg}.

For the fuzzy inference system, the membership functions of normalized input variables are shown in Fig. 3, three fuzzy sets are proposed for each one, which are defined as Small (S), Medium (M), and Big (B), respectively. The membership function of the normalized output variable is shown in Fig. 4, seven fuzzy sets are considered for the output variable, which is defined as Very Small (VS), Small (S), Small Medium (SM), Medium (M), Big Medium (BM), Big (B), and Very Big (VB).

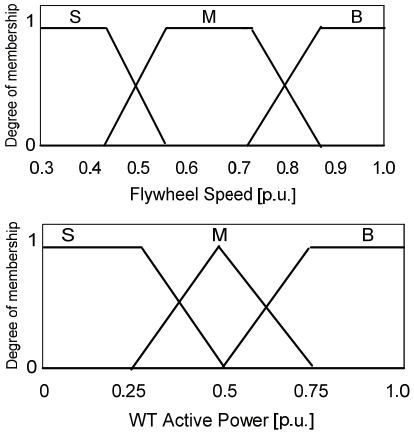

Fig.3. Membership degree of the input variables

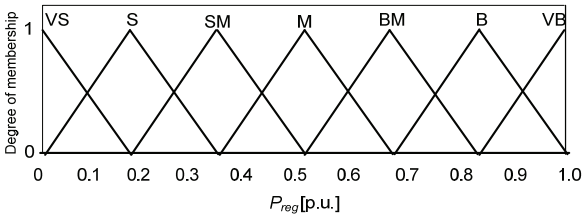

Fig.4. Membership degree of the output variable

According to the state of flywheel and the active power produced by WT, the active power expected from the coupling WT-FPC is inferred by the fuzzy logic inference system. The basic principles as following: If the flywheel speed is too small, the storage is favored, most of the generated power is used to charge the FPC, and a less power is delivered to the power grid. If this speed becomes too high, the restitution is selected. Then, if the speed is medium, the system operates normally. Therefore, the fuzzy logic inference rules are shown in Tab. 1.

Tab.1. Fuzzy logic inference table

ω_{rf} \ P_{wgf}	Small	Medium	Big
Small	VS	SM	BM
Medium	S	M	B
Big	SM	BM	VB

B. UC for the reactive power

The reactive power of FPC is controlled to maintain the stability of machine terminal voltage. As discussed above, the external bus is an infinite bus system, that is, $\dot{u}_b$ can be considered as an invariable vector with the phase angle equal to zero. According to Section 2.3, the machine terminal voltage fluctuates with the fluctuation of the active powers, P_g and P_{load}, and the reactive powers, Q_g and Q_{load}. According to Fig.1, the power equation of AC bus can be expressed by

(16)
$$\begin{cases} P_f + P_s = P_g + P_{load} \\ Q_f + Q_s = Q_g + Q_{load} \end{cases}$$

where P_f, P_{load} and Q_f, Q_{load} are the active powers and the reactive powers of GSC and local load.

For P_f and P_s are always fluctuating, and Q_f is controlled at the unity power factor usually, a PI controller with machine terminal voltage V_s as the feedback signal is designed to regulate the FPC reactive power Q_s to maintain the voltage stable, as shown in Fig.2.

3.2 Controller for GSC

The active power balance equation of the DC-link capacitor between the RSC and GSC shown in Fig.1 can be expressed by

(17)
$$P_{wg} - P_r - P_f = \frac{C}{2}\frac{d}{dt}V_{dc}^2$$

where P_r is the active power of FPC rotor, C is the capacitor value, and V_{dc} is the DC-link voltage. According to Equ.17, if P_f can be effectively controlled, the DC-link voltage V_{dc} can be maintained at the reference value V_{dcref}.

The control block diagram of the GSC of the studied system is shown in Fig.5. The *d*- and *q*-axis currents of the GSC, i_{gd} and i_{gq}, have to track the reference points that are determined by the active power P_f to maintain the DC-link voltage at the setting value and the reactive power to keep the output of GSC at a certain power factor, respectively. Considering the capacity of GSC, the reactive power of GSC is controlled at the unity power factor, i_{gqref} is set to zero. The required voltage of GSC is derived by controlling the *d*- and *q*-axis currents of GSC.

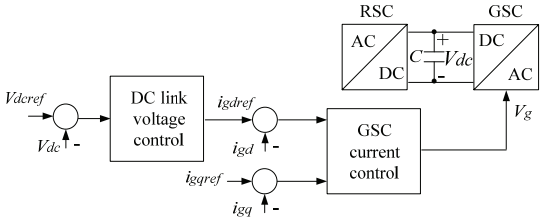

Fig.5. Control block diagram for the GSC

4. Simulation and discussion

Dynamic simulations are carried out in Matlab/Simulink platform to observe the responses of FPC to the variation of wind speed. All the simulation results run with the 250s duration with the same wind speed profile shown in Fig.6, and the results are shown in Fig.7-12.

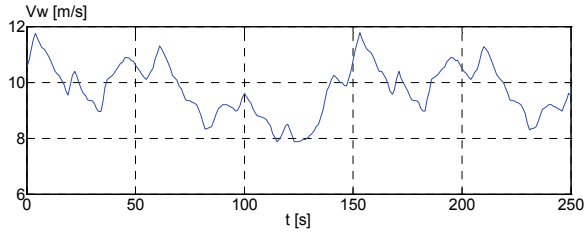

Fig.6. Wind speed Profile

The curve in Fig.7 shows the effectiveness of the controller for the DC-link voltage, the voltage is maintained at the setting value chosen here equal to 1 pu. Fig.8 is the speed curve of the flywheel, which demonstrates the operation state of FPC, absorbing or releasing the power. By contrast with Fig.6, it is seen that FPC absorbs the power and the flywheel accelerates when the wind speed is high, on the contrary, the FPC releases the power and the flywheel decelerates when the wind speed is low. Meanwhile, the flywheel rotational speed remains between the accepted limits always.

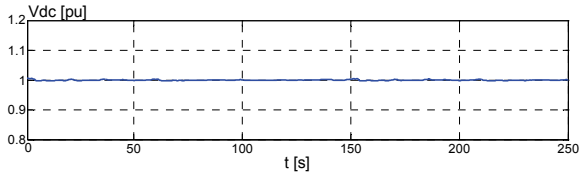

Fig.7. DC-link voltage curve

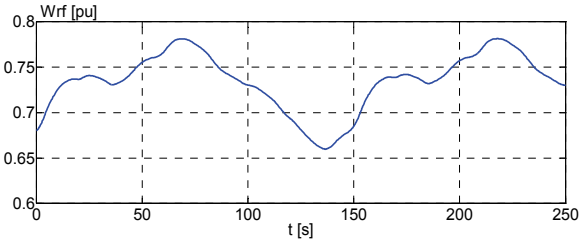

Fig.8. Flywheel speed curve

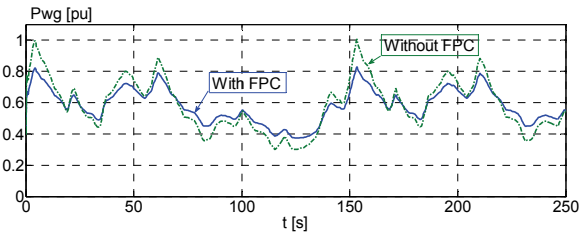

Fig.9. Active powers generated by the WT with and without FPC

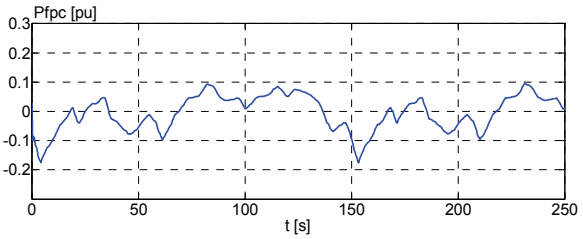

Fig.10. Active power generated by FPC

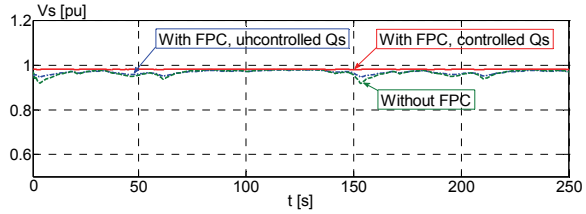

Fig.11. Machine terminal voltage curve under different conditions

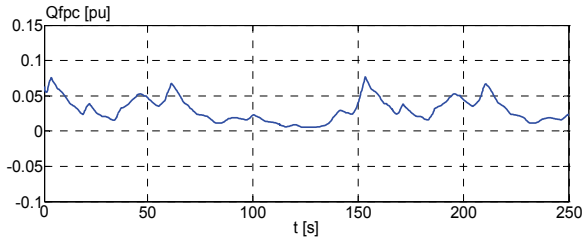

Fig.12. Reactive power generated by FPC

Fig. 9 shows the active powers generated by WT and WT-FPC fluctuate with the wind speed variation. When there is no FPC, the active power fluctuates heavily under the MPPT control strategy. While the WT associated with

FPC, the power fluctuation is comparatively smoother than without FPC, so the active power output characteristic of WT is enhanced effectively. The active power absorbed or released by FPC is shown in Fig. 10.

Fig. 11 is the machine terminal voltage profiles. From the profiles, it is seen that the machine terminal voltage fluctuation is reduced in a degree when the FPC is associated to the WT and its active power is controlled by fuzzy logic power supervisor. What's more, if the reactive power of FPC is also controlled properly, the machine terminal voltage can maintain at the setting value precisely. The reactive power generated by FPC is shown in Fig.12. The simulation results demonstrate that the power output characteristics of WT are well improved with the FPC cooperating with it.

6. Conclusion

This paper presents a novel configuration and operation control strategy of a DFIG based FESS associated to a WT connected to the power grid. In this configuration, because the main power exchanged between FESS and power grid is though the stator of DFIG, and one converter for DFIG is omitted, the cost of converters is reduced considerably. Meanwhile, for the FESS can directly regulate not only the active power but also the reactive power of WT, the active power and voltage characteristics of WT can be improved simultaneously. The control strategy that the active power of the associated system is regulated based on a fuzzy logic inference system and the machine terminal voltage is controlled by regulating the reactive power of FESS, is proposed. The simulation results verify the effectiveness of the proposed configuration and control strategy.

Acknowledgements: This work was supported by the National Natural Science Foundation of China (50937002), the Natural Science Foundation of Hubei Province in China (2009CDA042), and the National Basic Research Program of China (2009CB219702).

Appendix

Parameters of the studied system in per unit (pu)

Wind turbine	Based power S_{base}	1.5MW
	Rated power S_{rated}	1.5MW
	Stator resistor R_{sw}	0.02
	Stator inductance L_w	0.5
	Magnet flux ψ_w	1.1
	Pole-pair number p_w	30
	Rotating Inertia J_w	40
	Friction coefficient M_w	0.0012
	DC-link voltage Vdc	1
FPC	Stator resistor R_s	0.00706
	Rotor resistor R_r	0.0045
	Stator inductance L_s	1.441
	Rotor inductance L_r	1.317
	Mutual inductance L_m	1.168
	Pole-pair number p_f	3
	Rotating Inertia J_f	300
Tie-line	Resistor R_l	8.2
	Inductance X_l	4.2
Local load	Resistor R_{load}	0.02
	Inductance X_{load}	0.4
Power grid	Grid voltage V_b	1
	Syachronous speed ω_1	1

REFERENCES

[1] LU M. S.，Chang C. L., Lee W. R.，et al, Combining the wind power generation system with energy storage equipment, IEEE Trans. on Ind. Appli.，45 (2009)，No. 6, 2109-2115

[2] Hebner R., Beno J., Walls A., Flywheel Batteries Come Around Again. IEEE Spectr., 39 (2002), No. 4, 46-51

[3] Wang M. H., Chen H. C., Transient Stability Control of Multi-machine Power Systems Using Flywheel Energy Injection. IET Proc. Gener. Transm. Distrib., 152 (2005), No. 5, 589-596

[4] Cardenas R., Pena R., Asher G., Clare J., Control Strategies for Enhanced Power Smoothing in Wind Energy Systems using a Flywheel Driven by a Vector-Controlled Induction Machine. IEEE Trans. Ind. Electron., 48 (2001) No. 3, 625-635

[5] Gabriel O. C., Christophe S., et al, Control and Performance Evaluation of a Flywheel Energy-Storage System Associated to a Variable-Speed Wind Generator, IEEE Trans. Ind. Electron., 53 (2006) No. 4, 1074–1085

[6] Cardenas R., Pena R., et al, Control Strategies for Power Smoothing using a Flywheel Driven by a Sensorless Vector-Controlled Induction Machine Operating in a Wide Speed Range, IEEE Trans. Ind. Electron., 51 (2004) No. 3, 603–614

[7] Cardenas R., Pena R., et al, Power Smoothing using a Flywheel Driven by a Switched Reluctance Machine, IEEE Trans. Ind. Electron. 53 (2006) No. 4, 1086–1093

[8] Lukic S. M., Jian C., et al, Energy Storage Systems for Automotive Applications, IEEE Trans. Ind. Electron. 55 (2005) No. 6, 2258–2267

[9] Kenny B. H., Jansen R., et al, Integrated Power and Attitude Control with Two Flywheels, IEEE Trans. Aerospace and Electronic Systems, 41 (2005) No. 4, 1431–1449

[10] Lazarewicz M. L., Rojas A., Grid Frequency Regulation by Recycling Electrical Energy in Flywheels, Power Engineering Society General Meeting 2004 (2004), 2038–2042

[11] Barton J. P., Infield D. G., Energy storage and its use with intermittent renewable energy. IEEE Trans. Energy Convers., 19 (2004), No. 2, 441-448

[12] Hilmar, D., Comparison of High-Power Short-Term Flywheel Storage Systems, the 21st Int. Telecommunication Energy Conf, Copenhagen, Denmark, Jun., 1999

[13] Christof S., Amir M. M., A Stabilizer for Oscillating Torques in Synchronous Machines, IEEE Trans. Ind. Appl., 41 (2005) No. 3, 748–755

[14] LI R., Xiang D. W., Kirtley J. L., Analysis of Electromechanical Interactions in a Flywheel System with a Doubly Fed Induction Machine, IEEE Trans. on Ind. Appl., 47 (2011) No.3, 1498-1506

[15] Hirofumi A., Hikaru S., Control and Performance of a Doubly-Fed Induction Machine Intended for a Flywheel Energy Storage System, IEEE Trans. Power Electr. 17 (2002) No. 1, 109–116

[16] Muller S., Deicke M., De Donchker R. W., Doubly Fed Induction Generator Systems for Wind Turbine, IEEE Ind. Appl. Mag., 8 (2002) No.3, 26–33

[17] Monica C., Santiago A., Juan C. B., Control of Permanent-Magnet Generators Applied to Variable-Speed Wind-Energy Systems Connected to the Grid, IEEE Trans. Energy Convers., 21 (2006) No. 1, 130–135

[18] Wang L., Yu J. Y., Chen Y. T., Dynamic Stability Improve of an Integrated Offshore Wind and Marine-current Farm using a Flywheel Energy-storage System, IET Renew. Power Gener., 5 (2011), No. 5, 387-396

[19] Ekanayake J. B., Holdsworth L., et al, Dynamic Modeling of Doubly Fed Induction Generator Wind Turbines, IEEE Trans. Power Systems, 18 (2003), No. 2, 803–809

[20] Lilia J.，Lotfi K.，Abderrazak O., A Fuzzy Logic Supervisor for Active and Reactive Power Control of a Variable Speed Wind Energy Conversion System Associated to a Flywheel Storage System, Electric Power Systems Research，79(2009), 919-925

***Authors**: Shilin LIU, Prof. Jinyu WEN, and Prof. Shaorong WANG are with the State Key Laboratory of Advanced Electromagnetic Engineering and Technology, Huazhong University of Science and Technology, Luoyu Road 1037, Wuhan City, Hubei Province, P. R. China, E-mail: Shlin.Liu@hotmail.com*